ELSEVIER

Contents lists available at ScienceDirect

LITHOS

journal homepage: www.elsevier.com/locate/lithos





Pre-eruptive water content and volatile degassing processes in the southern Okinawa Trough magma: Implications for subduction zone water recycling and magmatic contributions to hydrothermal systems

Yuxiang Zhang ^{a,b,c,d,*}, Glenn Gaetani ^c, Brian Monteleone ^c, Zhigang Zeng ^{a,b,d,*}, Zuxing Chen ^{a,b,d}, Xuebo Yin ^{a,b,d}, Xiaoyuan Wang ^{a,b,d}, Shuai Chen ^{a,b,d}

- a Key Laboratory of Marine Geology and Environment, Institute of Oceanology, Chinese Academy of Sciences, Qingdao 266071, China
- b Laboratory for Marine Mineral Resources, Qingdao National Laboratory for Marine Science and Technology, Qingdao 266071, China
- ^c Department of Geology and Geophysics, Woods Hole Oceanographic Institution, Woods Hole 02543, USA
- ^d Center for Ocean Mega-Science, Chinese Academy of Sciences, Qingdao 266071, China

ARTICLE INFO

Keywords: Volatile Water recycling Serpentinite Magma degassing Seafloor hydrothermal system

ABSTRACT

Volatiles can act as a critical link that connects the magmatic and hydrothermal systems in subduction zones. Here, we present the first analyses of volatile (e.g., H2O, CO2, and S) concentrations in melt inclusions and matrix glasses of volcanic rocks from a modern arc front volcano (Irabu Knoll) and two back-arc spreading centers (Yaeyama Graben and Yonaguni Graben) in the southern Okinawa Trough, a nascent back-arc basin that is characterized by widespread volcanic and hydrothermal activity. The pre-eruptive H₂O concentrations of magmas (~2.2 to ~3.1 wt%) were estimated using a combination of melt inclusion analyses and plagioclase-melt hygrometry. From the back-arc to the arc, the H_2O/Ce of lavas increase monotonically with the increasing $\delta^{11}B$ values, a good geochemical tracer for subducted serpentinites. By combining our data with those from other subduction zones (Mariana Arc, Mariana Trough, Tonga Arc, Lau Basin) and MORB, we established a robust correlation between H_2O/Ce and $\delta^{11}B$, suggesting that subducted serpentinites might have a significant contribution to the water budget of arc magmas. The low CO₂ concentrations in our melt inclusions (~45–225 µg/g, after vapor bubble correction) and matrix glasses ($<1 \,\mu g/g$, below detection limit) as compared to $>3000 \,\mu g/g$ in primary arc magmas, suggests that significant CO2 degassing has occurred during magma ascent and/or in the magma reservoir, which can release sufficient CO₂ to support the high CO₂ flux of the hydrothermal system in the Okinawa Trough. This also implies that hydrothermal CO2 in this area is not likely derived from fluid-rock interactions. In addition, the concentration of S in the magma decreases with the progressive loss of H₂O, whereas the concentrations of F and Cl remain constant. Our results thus suggest that magma degassing is a potentially important source of CO2, S, and H2O to the hydrothermal system in the Okinawa Trough.

1. Introduction

At subduction zones, fluids released from the subducting hydrated slab trigger partial melting of the mantle wedge and produce magmas that are enriched in $\rm H_2O$ and other volatiles (e.g., S, F, Cl) compared to those generated beneath mid-ocean ridges (Kendrick et al., 2020; Sobolev and Chaussidon, 1996; Wallace, 2005; Zellmer et al., 2015). Those volatile species could be transferred to the shallow crust or degassed to the ocean or atmosphere during magma ascent (Butterfield et al., 2011; Edmonds and Mather, 2017; Wallace, 2005; Webster et al.,

1999). Of particular interest is that magmatic volatiles act as a link between magmatic and hydrothermal systems. Many researchers have suggested that magmatically derived fluids can not only contribute to the chemistry of hydrothermal fluids (e.g., Herzig et al., 1998; Reeves et al., 2011; Seewald et al., 2015; Seewald et al., 2019; Yang and Scott, 2005), but also carry a significant amounts of metals (e.g., Cu, Zn) to the hydrothermal system (e.g., Kim et al., 2011; Marques et al., 2011; Yang and Scott, 1996; Yang and Scott, 2002). Therefore, decoding the volatile compositions of arc or back-arc magmas is of great importance for understanding the chemical exchange between magmatic and

^{*} Corresponding authors at: Key Laboratory of Marine Geology and Environment, Institute of Oceanology, Chinese Academy of Sciences, Qingdao, China. E-mail addresses: zhangyuxiang13@mails.ucas.ac.cn (Y. Zhang), zgzeng@qdio.ac.cn (Z. Zeng).

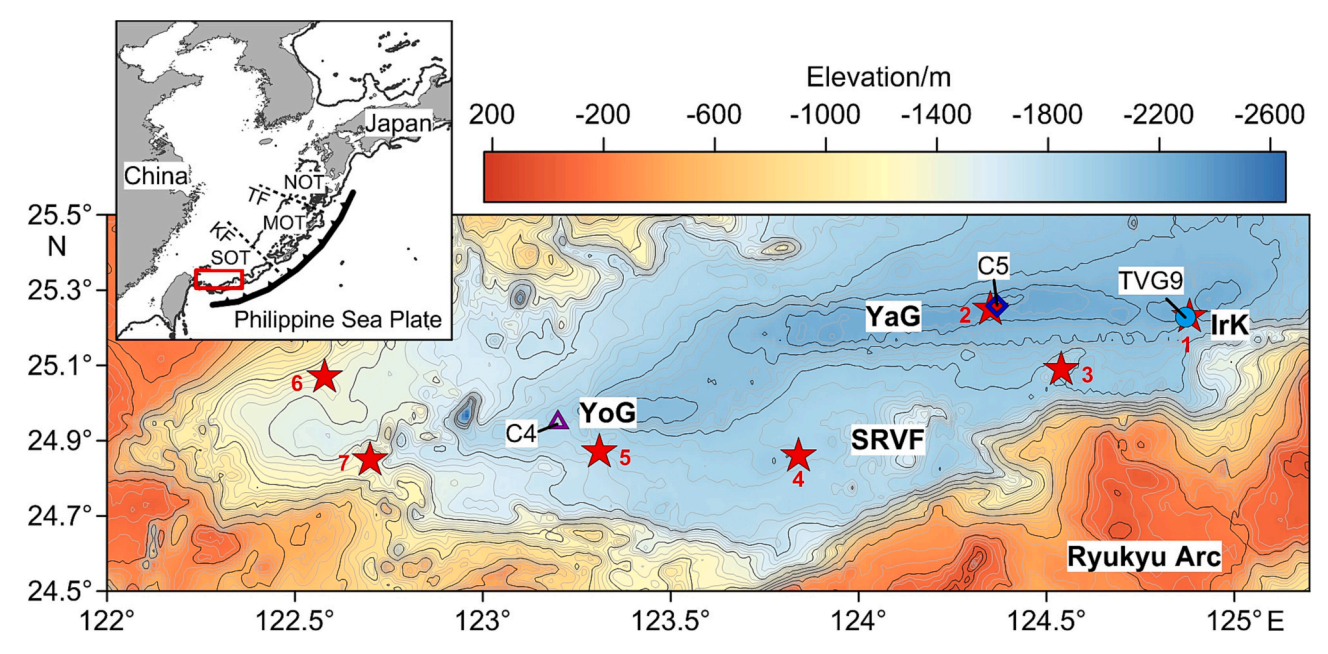


Fig. 1. Bathymetric map of the southern Okinawa Trough (SOT) showing the sampling locations. The red rectangle in the inset delineates the area covered by the large map. The red stars indicate the locations of hydrothermal sites: 1-Irabu Knoll, 2-Yokosuka, 3-Tarama Knoll, 4-Hotoma Knoll, 5-Futagoyama, 6-Tangyin, 7-Yonaguni Knoll IV (http://vents-data.interridge.org/). Abbreviations: IrK-Irabu Knoll, YaG-Yaeyama Graben, YoG-Yonaguni Graben, SRVF-southern Ryukyu Volcanic Front, NOT-northern Okinawa Trough, MOT-middle Okinawa Trough, KF-Kerama fault, TF-Tokara fault. (For interpretation of the references to colour in this figure legend, the reader is referred to the web version of this article.)

hydrothermal system in subduction zones.

The Okinawa Trough is a young back-arc basin developed behind the Ryukyu arc-trench system (Fig. 1). Results from recent studies have elucidated the influence of subduction input of sediments, altered oceanic crust (AOC), and serpentinite on the Okinawa Trough lavas, which show enrichment of large ion lithosphere elements (LILE) and radiogenic Sr-Nd-Pb-Hf (e.g., Guo et al., 2017; Shinjo et al., 1999; Shu et al., 2017; Zhang et al., 2021a; Zhu et al., 2021). However, one key indicator for the recycling of subduction fluids—the pre-eruptive H₂O concentrations of the Okinawa Trough magmas—remains unknown. In addition, the Okinawa Trough has intense and widespread hydrothermal activity. The hydrothermal fluids in this area are characterized by high concentrations of CO₂ (up to ~200 mmol/kg), which is suggested to come from magma degassing or interactions between fluid and volcanogenic sediment (Gamo et al., 2006; Ishibashi et al., 2014; Kawagucci et al., 2011; Konno et al., 2006; Miyazaki et al., 2017; Sakai et al., 1990). Sulfur and noble gas isotopes of hydrothermal products also indicate a direct contribution of volatiles from the magmatic system (Hou et al., 2005; Ishibashi and Urabe, 1995; Sakai et al., 1990; Yang et al., 2020). Despite this understanding of magmatic-hydrothermal relations in the Okinawa Trough, knowledge about the degassing behavior of volatiles in the sub-volcanic magma reservoir is lacking.

The Yaeyama and Yonaguni Grabens are active back-arc spreading centers in the southern part of the Okinawa Trough. The Irabu Knoll is a submarine volcano belonging to the southern Ryukyu volcanic front, which is a volcanic chain that is geographically located in the southern Okinawa Trough but actually represents the modern arc volcanism (Sibuet et al., 1998). Hydrothermal activities have been reported in these areas (Fig. 1). A previous study has shown that the arc magmas are influenced by more slab-derived fluids than the back-arc magmas (Zhang et al., 2021a). In this contribution, we estimated the pre-eruptive H₂O concentrations in the magmas of Irabu Knoll, Yaeyama Graben, and Yonaguni Graben through a combination of melt inclusion analyses and plagioclase-liquid hygrometry, with a goal of assessing the influence of subduction input on the cross-arc variation in the water budget of the southern Ryukyu subduction zone. Furthermore, we analyzed the volatile (H₂O, CO₂, S, F, Cl) concentrations in phenocryst-hosted melt

inclusions and matrix glasses of volcanic lavas from the Irabu Knoll to address the degassing behavior of volatiles in the sub-volcanic reservoir and the possible magmatic contributions to the hydrothermal system.

2. Geological settings

The Okinawa Trough is located on the eastern margin of the Asian continental lithosphere (Fig. 1). It developed through back-arc extension occurring behind the Ryukyu Arc since the Middle Miocene, in response to the subduction of the Philippine Sea Plate (Sibuet et al., 1998). The back-arc basin is divided into northern, middle, and southern segments by the Tokara fault and Kerama fault (Fig. 1). Volcanism associated with basin extension occurs within several *en echelon* linear central grabens in the middle and southern segments. A long volcanic belt that is mainly composed of a series of submarine volcanoes or volcanic islands representing the modern arc volcanism is located on the eastern side of the trough (Sibuet et al., 1998). Volcanic rocks sampled from the Okinawa Trough have young ages (mostly <1 Ma; Chen et al., 2018; Shinjo et al., 1999; Shinjo and Kato, 2000) and have a bimodal distribution dominated by basalts and rhyolites (Shinjo et al., 1999; Shinjo and Kato, 2000; Zhang et al., 2018; Zhang et al., 2020).

During the last three decades, >15 active hydrothermal sites have been discovered in the middle and southern segments of the Okinawa Trough (http://vents-data.interridge.org/). Hydrothermal fluids in these areas are characterized by higher concentrations of CO_2 , CH_4 , NH_4^+ , and K compared to those in sediment-starved mid-ocean ridge hydrothermal systems (Gamo et al., 2006; Ishibashi et al., 2014; Kawagucci et al., 2011; Konno et al., 2006; Miyazaki et al., 2017; Sakai et al., 1990). Hydrothermal sulfides in the Okinawa Trough are enriched in Cu, Cu,

The Yaeyama and Yonaguni Grabens are two nearly EW trending central grabens that mainly erupt basalts and basaltic andesites in the southern Okinawa Trough (Shinjo et al., 1999; Shu et al., 2017). The Yaeyama Graben is the deepest part of the trough (<-2000 m) and has the thinnest crust (<10 km) and, thus, represents the highest degree of back-arc extension (Arai et al., 2017; Nishizawa et al., 2019). High

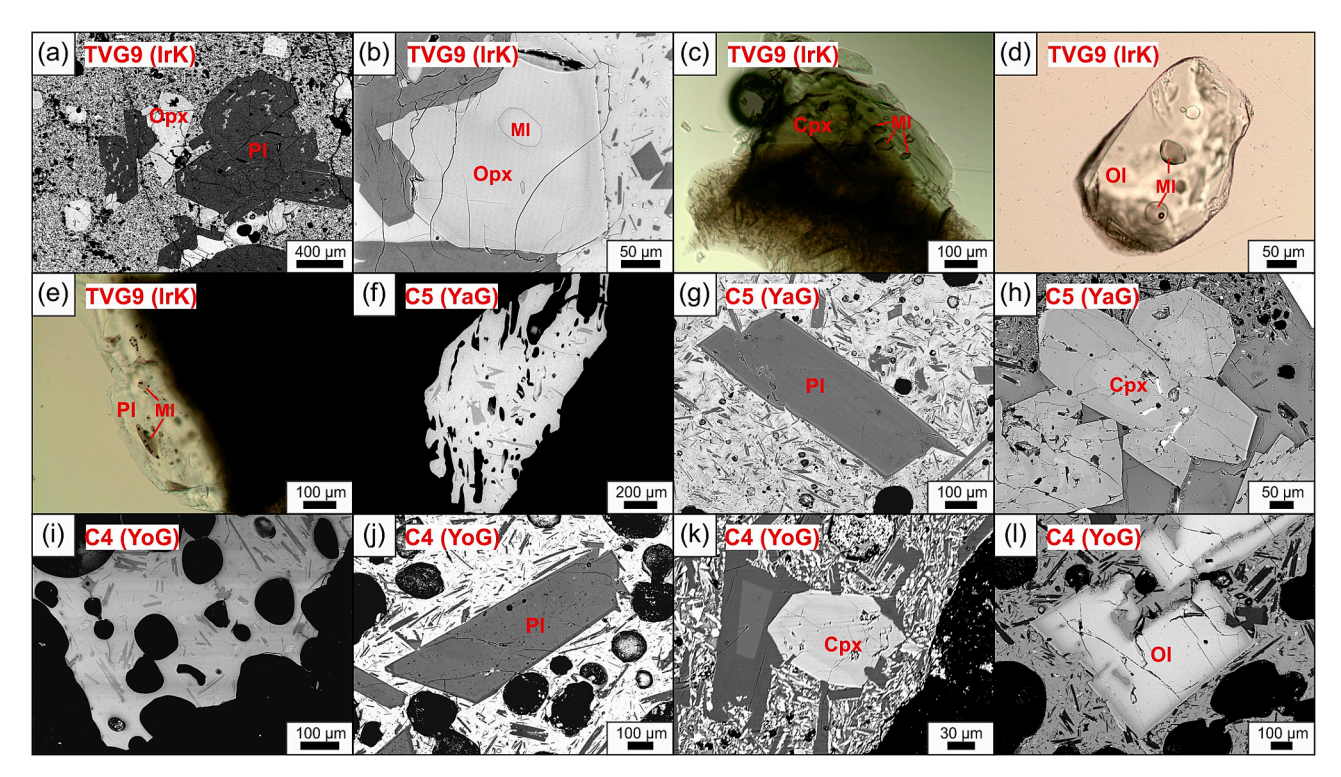


Fig. 2. Photomicrographs of phenocrysts and glasses for the Irabu Knoll (IrK-TVG9) samples (a-e), Yaeyama Graben (YaG-C5) samples (f-h), and Yonaguni Graben (YoG-C4) samples (i-l). TVG9 samples have abundant plagioclase (Pl), orthopyroxene (Opx), clinopyroxene (Cpx), and olivine (Ol) phenocrysts, which all contain glassy melt inclusions (MI). C5 and C4 samples are mainly composed of glasses and microlites and they contain very small amount of MI-free phenocrysts.

temperature and CO_2 -rich hydrothermal fluids are venting from the central part of the Yaeyama Graben (Yokosuka site; Miyazaki et al., 2017). The Irabu Knoll, mainly composed of basaltic rocks, is located on the northeastern end of the southern Ryukyu Volcanic Front, and the eastern edge of the Yaeyama Graben. It consists of three major seamounts: East, West, and South seamounts; clear hydrothermal fluid venting was found at the summit of the West seamount (Fukuba et al., 2015).

3. Samples and methods

Samples are fresh basaltic andesites collected from the Yaeyama Graben (C5), Yonaguni Graben (C4), and Irabu Knoll (TVG9), using a television sampler during the "HOBAB4" cruise of R/V KEXUE in 2016. Sampling locations are shown in Fig. 1. The whole-rock geochemical data of these samples are given by Zhang et al. (2021a). Both the Yaeyama Graben samples and Yonaguni Graben samples are glassy lavas that mainly composed of microlites (plagioclase, pyroxene, and olivine) and matrix glass (Fig. 2f and i). They also contain a limited amount of large phenocrysts (mainly plagioclase and clinopyroxene); no melt inclusions exist in these phenocrysts (Fig. 2g-I). The Irabu Knoll samples (TVG9) have much higher degree of crystallinity with abundant phenocrysts including plagioclase, orthopyroxene, clinopyroxene, and olivine; some phenocrysts contain glassy melt inclusions (Fig. 2b-e).

Phenocrysts (olivine, plagioclase, and pyroxene) that contain glassy melt inclusions were hand-picked from the crushed rock fragments, mounted in epoxy, and polished to expose the inclusions. Some fragments (1–2 mm) of matrix glass were also mounted in epoxy and polished for microanalysis. Polished phenocrysts and glass chips were removed from epoxy and remounted in indium metal to minimize volatile backgrounds during secondary ion mass spectroscopy (SIMS) analysis. These mounts were cleaned in an ultrasonic bath using ethanol followed by ultrapure water, and then coated with Au for SIMS analysis. Thin sections were also prepared and coated with carbon for electron microprobe analysis (EMPA).

The major element compositions of the phenocryst, matrix glasses, and melt inclusions were determined by a JEOL JXA-8230 electron microprobe analyzer equipped with three wavelength dispersive spectrometers at the Ocean University of China. An accelerating voltage of 15 kV was used for quantitative analyses. A beam current of 20 nA and a spot diameter of 2–5 μm were used for mineral analyses. For glass analyses, the beam current was decreased to 10 nA and the spot diameter was increased to 10–15 μm to reduce the migration of Na. Na and K were measured first in each analysis, with 10 s as the peak counting time and 5 s as the background counting time. The standards used for the calibration included diopside for Mg, Si, and Ca; albite for Na; pyrope garnet for Al; hematite for Fe; sanidine for K; rutile for Ti; chromium oxide for Cr; and bustamite for Mn. The relative analytical precision for the major elements was better than 1%.

Volatile concentrations (H2O, CO2, F, Cl, and S) of the matrix glasses and melt inclusions were determined by SIMS using the Cameca IMS 1280 ion microprobe at the Northeast National Ion Microprobe Facility at Woods Hole Oceanographic Institution. A ¹³³Cs⁺ beam, with a primary current of 10 \pm 0.5 nA and an accelerating voltage of 10 kV, was used for volatiles analyses. The beam was rastered over a 30 \times 30 μ m² area. The secondary field aperture was set to 406 μ m. The field aperture is in the secondary ion stream and blocks the transmission of secondary ions from outside of the innermost $5 \times 5 \mu m^2$ of the sputtering crater during analysis. This is critical for keeping contribution of surface volatiles low. Long pre-sputtering, relatively strong primary beam (10 nA current), and field aperture are necessary to reduce background contribution. Each measurement consists of a 240 s pre-sputtering period followed by 5 cycles of collection of ¹²C⁻, ¹⁶O¹H⁻, ¹⁹F⁻, ³⁰Si⁻, $^{32}\mathrm{S}^-$, and $^{35}\mathrm{Cl}^-$ with a mass resolving power (MRP) of \sim 6700, sufficient to separate the ¹⁷O⁻ peak from ¹⁶O¹H⁻. Calibration for volatiles was done on a series of standards (519-4-1, 46D, D52-5, D51-3, 1649-3, D20-3, D30-1, JD17H, 6001, 1654-3, NS-1). The calibration lines are presented in Fig. S1. Background corrections were done using analyses of volatile-free materials (synthetic forsterite for Cl, suprasil for other volatiles). Analytical uncertainties on individual volatile concentration

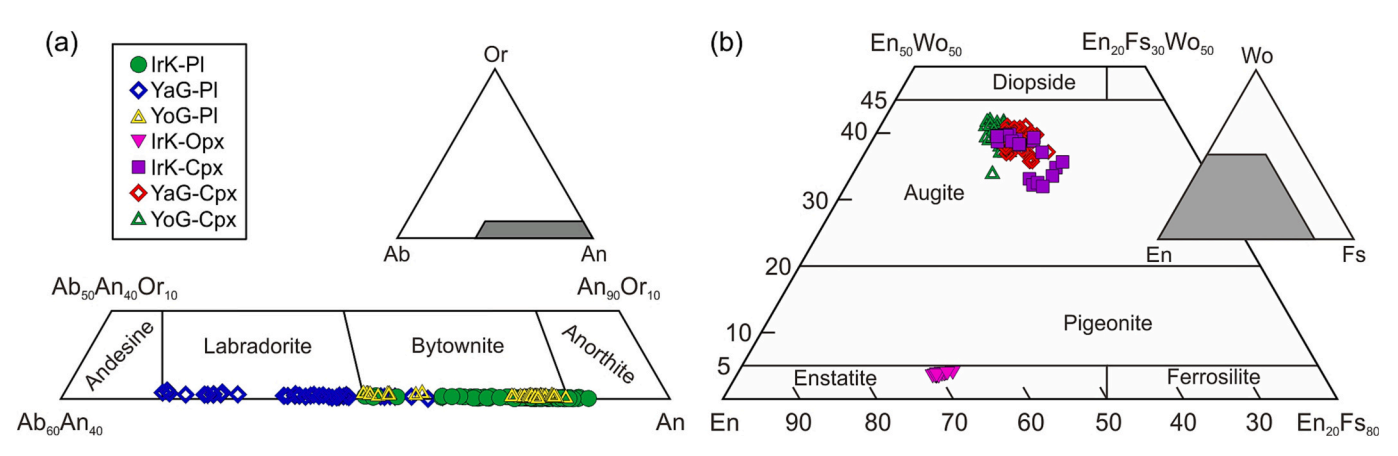


Fig. 3. Classification diagrams for the plagioclase phenocrysts (a) and pyroxene phenocrysts (b) in the lavas from the southern Okinawa Trough. Abbreviations: IrK-Irabu Knoll, YaG-Yaeyama Graben, YoG-Yonaguni Graben.

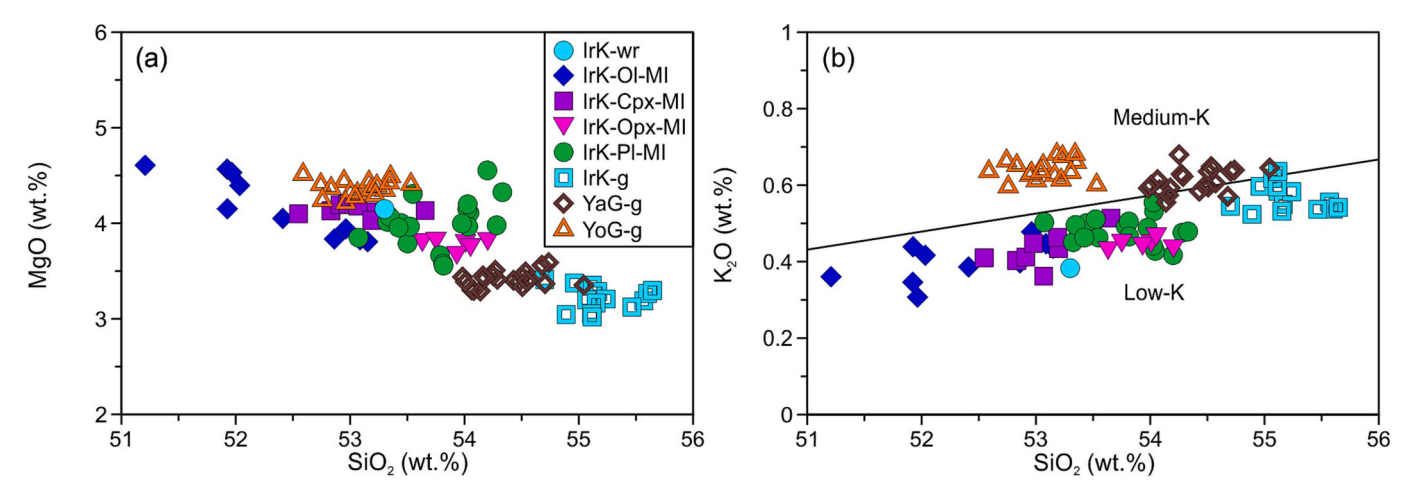


Fig. 4. Plots of MgO versus SiO₂ (a) and K₂O versus SiO₂ (b) for the melt inclusions and matrix glasses in the southern Okinawa Trough lavas. Abbreviations: IrK-Irabu Knoll, YaG-Yaeyama Graben, YoG-Yonaguni Graben.

measurement are $<\!3\%$ for $CO_2\left(2\,\sigma\right)$ and $<\!2\%\left(2\,\sigma\right)$ for $H_2O,\,F,\,S,$ and Cl. Errors on calibration slopes, determined by bootstrap regression of standard measurement data, ranged from 2 to 6% (2 σ) among the volatiles for each session.

4. Results

4.1. Major element compositions of phenocrysts

Major element compositions of plagioclase, clinopyroxene, orthopyroxene, and olivine phenocrysts are given in Tables S1-S4. Plagioclase phenocrysts were observed in all the samples and most are euhedral (Fig. 2a, g, and j). The plagioclase phenocrysts in Irabu Knoll samples are large (up to 2 mm) and have high An values (70–92, where An = molar Ca/ (Ca + Na + K) \times 100). The plagioclase phenocrysts from Yonaguni Graben samples are smaller (~0.2–1 mm) with similarly high An values (70–90). In comparison, those in Yaeyama Graben samples (~0.2–0.8 mm) have much lower An values (50–77) (Fig. 3a). All the plagioclase phenocrysts have low-An rims (~70–80 in Irabu Knoll and Yonaguni Graben and ~50–60 in Yaeyama Graben samples).

Clinopyroxene phenocrysts were also observed in all the samples and have subhedral to euhedral crystal shapes (Fig. 2a, h, and k). The Irabu Knoll clinopyroxene phenocrysts ($\sim\!0.2\text{--}1$ mm) have Mg# values of 63–77 (Mg# = 100 \times molar Mg/(Mg + Fe $_{tot}$)), similar to those in Yonaguni Graben (Mg# = 73–79) and Yaeyama Graben (Mg# = 66–75) samples (Fig. 3b). Orthopyroxene phenocrysts only occur in Irabu Knoll

samples, with regular crystal shapes and Mg# values of 74–76 (Fig. 3b). The olivine phenocrysts in Irabu Knoll samples are anhedral to euhedral (\sim 0.1–0.5 mm) and have low Mg# values (69–71). Yonaguni Graben samples also contain large olivine phenocrysts (\sim 0.5–1 mm), which have slightly higher Mg# values (69–77). No olivine phenocrysts were observed in Yaeyama Graben samples.

4.2. Major elements and volatiles of melt inclusions and matrix glasses

The major element compositions and volatile (H₂O, CO₂, F, Cl, and S) concentrations of melt inclusions (Irabu Knoll) and matrix glasses (Irabu Knoll, Yonaguni Graben, and Yaeyama Graben) are given in Tables S5 and S6. The F and Cl data were reported by Zhang et al. (2021a). The melt inclusions hosted in plagioclase and orthopyroxene are slightly more evolved than those in olivine and clinopyroxene (Fig. 4). Compositions of melt inclusion can be affected by post-entrapment crystallization (PEC) of host crystals onto the inclusion walls (Danyushevsky et al., 2002). To check whether our melt inclusions are influenced by this process, we assessed the equilibrium relations between the included melt and host phenocrysts, according to the following exchange coefficients from Putirka (2008): $K_D(Fe{--}Mg)^{Ol{\text -}liq}$ (0.299 \pm 0.053) for olivine, $K_D(An-Ab)^{Pl-liq}$ (0.10 \pm 0.05 at T <1050 °C; 0.27 \pm 0.11 at T >1050 °C) for plagioclase, $K_D(Fe-Mg)^{Cpx-liq}$ (0.28 \pm 0.08) for clinopyroxene, and $K_D(Fe-Mg)^{Opx-liq}$ (0.29 \pm 0.06) for orthopyroxene. Results show that the melt inclusions are all in equilibrium with their host minerals (Table S5), indicating that the effects of PEC are small. Thus, no

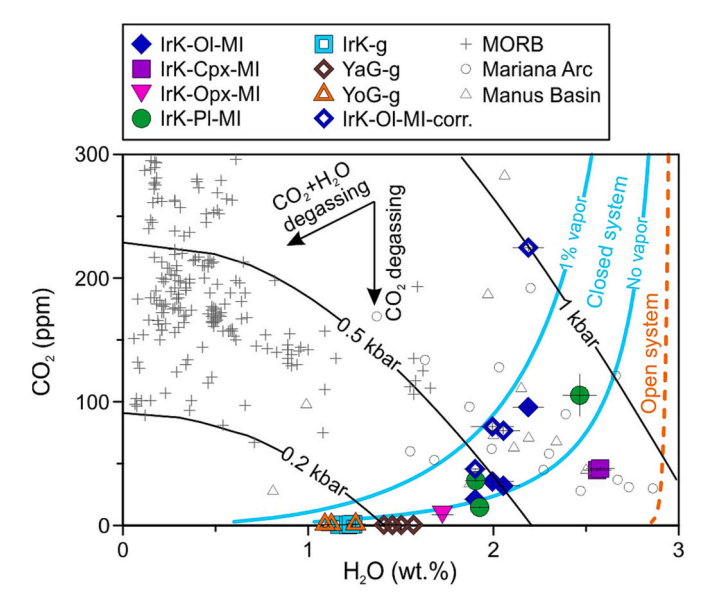


Fig. 5. Plots of CO₂ versus H₂O for the melt inclusions and matrix glasses in the southern Okinawa Trough lavas. Also shown are the data of MORB (htt ps://www.earthchem.org/petdb; data are obtained using SIMS methods), Mariana Arc (Shaw et al., 2008), and Manus Basin (Siegburg et al., 2018) for comparison. The CO₂ degassing behavior in subduction zone magmas is quite different from that in mid-ocean ridge magmas. The degassing paths and isobars are calculated using the VolatileCalc model of Newman and Lowenstern (2002). Abbreviations: IrK-Irabu Knoll, YaG-Yaeyama Graben, YoG-Yonaguni Graben.

PEC correction was applied to the volatile concentrations of melt inclusions.

H₂O concentrations in the melt inclusions range from 1.72 to 2.58 wt %, with the highest values recorded by the inclusions hosted in clinopyroxene and plagioclase. The olivine-hosted melt inclusions generally have lower H₂O concentrations (1.90-2.19 wt%), which is probably attributable to the diffusive loss of H through host olivine after entrapment (Bucholz et al., 2013; Gaetani et al., 2012). The melt inclusions have low CO₂ concentrations (8-105 µg/g); the low values are partly due to the presence of vapor bubbles (Fig. 2d and e), which can accommodate a significant amount of the total CO2 in the melt inclusion (e.g., ~40-90%; Moore et al., 2015; Wallace et al., 2015). We reconstructed the CO2 concentrations in the olivine-hosted melt inclusions following the bubble correction method of Rasmussen et al. (2020). The corrected CO₂ concentrations range from 45 μg/g to 225 μg/g (Fig. 5). S concentrations in the melt inclusions range from 397 to 772 µg/g. F and Cl concentrations in the melt inclusions show relatively small variations (215–288 μ g/g and 711–940 μ g/g, respectively).

The matrix glasses of Irabu Knoll and Yonaguni Graben samples have similar H_2O (~1.0–1.3 wt%) and S (~170–240 $\mu g/g$) concentrations, which are slightly lower than those in Yaeyama Graben glasses (H_2O ~ 1.5 wt%, S ~ 350 $\mu g/g$). Of particular note, the matrix glasses in all samples have extremely low CO_2 concentrations (<1 $\mu g/g$; below detection limit). F (232–297 $\mu g/g$) and Cl (740–884 $\mu g/g$) concentrations in the Irabu Knoll matrix glasses are much closer to those in the melt inclusions. The Yonaguni Graben glasses have slightly higher F (282–334 $\mu g/g$) and lower Cl (592–698 $\mu g/g$) concentrations. The Yaeyama Graben glasses have significantly higher Cl concentrations (1520–1748 $\mu g/g$) and slightly higher F concentrations (370–413 $\mu g/g$).

5. Discussion

5.1. Variation of H_2O concentrations in the southern Okinawa Trough magnas

5.1.1. Estimation of pre-eruptive H_2O concentrations

Matrix glasses are quenched melts that have undergone significant degassing during ascent and eruption. Thus, the analyzed H₂O concentrations in the matrix glasses cannot represent the pre-eruptive H2O concentrations in the magmas. Conversely, the phenocryst-hosted melt inclusions might be able to provide reliable constraints on the H2O budget in the southern Okinawa Trough magmas. Given that olivinehosted melt inclusions can experience H2O loss after entrapment (Bucholz et al., 2013; Gaetani et al., 2012), the highest H2O concentrations (~2.6 wt%) in the plagioclase- and clinopyroxene-hosted melt inclusions are likely closest to the pre-eruptive H₂O contents. However, the number of such melt inclusions are limited. As a supplementary method, we estimated the H₂O concentrations in the melt that is in equilibrium with plagioclase using the plagioclase-liquid hygrometer of Waters and Lange (2015), with the standard error estimate being 0.35 wt% H₂O for this method. The existence of plagioclase phenocrysts in all the samples makes it possible to investigate the cross-arc variation of H₂O concentrations in magmas of the southern Ryukyu subduction zone.

Temperature is an important input to the plagioclase-liquid hygrometer, but this hygrometer is insensitive to pressure (Waters and Lange, 2015). For example, for the plagioclase and melt compositions in this study, the estimated H2O concentrations remain unchanged when the pressure decreases from 2 kbar to 0.1 kbar. We adopted the clinopyroxene-melt (Eq. 33) and plagioclase-melt thermometers (Eq. 23) of Putirka (2008) to estimate liquidus temperatures, and the clinopyroxene-melt barometer (Eq. 31) of Putirka (2008) to estimate the crystallization pressures. Details of the calculations of temperatures and pressures are given in Table S7. These thermobarometers require knowledge of H₂O concentrations in the melt. For Irabu Knoll lavas, the melt inclusions with the highest H_2O concentrations (~2.6 wt%) in clinopyroxene and plagioclase were paired with their host minerals, yielding liquidus temperatures of 1038-1054 °C (average ~1050 °C) and a pressure of 0.4-1.1 kbar (Table S7). The vapor (H2O and CO2) saturation pressures estimated from the melt inclusions with highest H₂O and CO₂ concentrations are close to 1 kbar (Fig. 5). Because the vapor saturation pressures should represent the minimum values of the magma storage pressures, the crystallization pressures of the clinopyroxene and plagioclase crystals should be close to 1 kbar, indicating a shallow magma reservoir beneath the Irabu Knoll.

In order to get the H_2O concentrations as close to those in magmas prior to degassing as possible, the cores of large plagioclase phenocrysts were paired with the most primitive olivine-hosted melt inclusions, which are in equilibrium with the plagioclase cores (Fig. S2). Details of the calculations of H_2O concentrations are given in Table S8. The estimated H_2O concentrations in Irabu Knoll magmas are 2.9–3.1 wt%, which are slightly higher than the maximum values in the melt inclusions (~2.6 wt%). These values are close to the average primitive magma H_2O concentrations (3.3 \pm 1.2%) of global arc fronts (Ruscitto et al., 2012). However, as the Irabu Knoll melts have relatively low MgO contents (<5 wt%) and are nearly vapor saturated in the magma reservoir (Fig. 5), we cannot exclude the possibility of deep H_2O degassing of their parental magmas. Therefore, the H_2O concentrations of 2.9–3.1 wt% should represent the minimum values of primitive magmas beneath the Irabu Knoll.

For Yaeyama Graben and Yonaguni Graben lavas, the cores of plagioclase phenocrysts are in major element equilibrium with the whole-rock compositions [with the exception of C4 plagioclase, which is in equilibrium with a less evolved lava (2K-1177-4) from the Yonaguni Graben reported by Shu et al., 2017] (Fig. S2) and can be used to estimate pre-eruptive $\rm H_2O$ concentrations. However, the lack of melt inclusion $\rm H_2O$ data makes it difficult to estimate magma storage

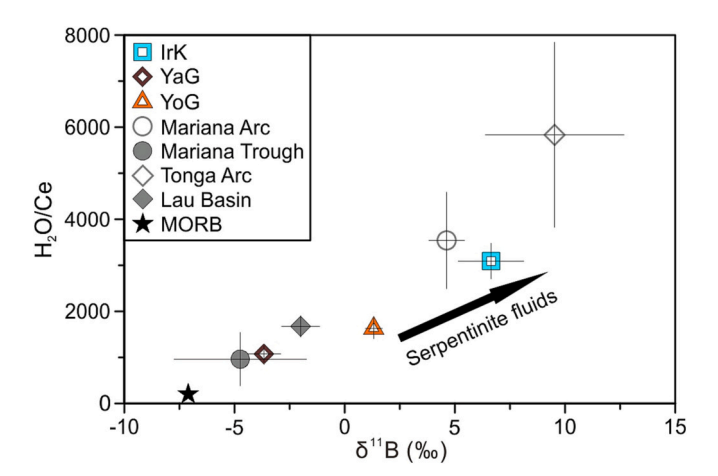


Fig. 6. Plots of $\rm H_2O/Ce$ versus $\rm \delta^{11}B$ for the lavas from the Irabu Knoll (IrK), Yaeyama Graben (YaG), and Yonaguni Graben (YoG). The average values of Mariana Arc, Mariana Trough, Tonga Arc, Lau Basin, and MORB are also presented for comparison. Error bars indicate 1 σ uncertainty. These data define a robust correlation between $\rm H_2O/Ce$ and $\rm \delta^{11}B$ ($\rm r^2=0.89$), suggesting that serpentinite fluids play a significant role in water recycling in subduction zones. The average $\rm H_2O/Ce$ values (except for those obtained in this study) are from Ruscitto et al. (2012). $\rm \delta^{11}B$ data sources: southern Okinawa Trough (Zhang et al., 2021a), Mariana Arc (Ishikawa and Tera, 1999), Mariana Trough and Lau Basin (Chaussidon and Jambon, 1994; Chaussidon and Marty, 1995), Tonga Arc (Leeman et al., 2017), MORB (Marschall, 2018).

temperatures using the clinopyroxene- and plagioclase-based thermometers. These samples are mainly composed of microlites (Fig. 2f and i), suggesting that the magmas ascended rapidly. We assumed that magma ascent is an adiabatic process and calculated the liquidus temperatures using plagioclase phenocryst rims in equilibrium with the matrix glasses (Fig. S2), for which H₂O concentrations have been measured by SIMS. The results are 1110-1112 °C for Yonaguni Graben lavas and 1067-1075 °C for Yaeyama Gragen lavas (Table S7). The pressure was assumed to be 1 kbar. Based on these values, the plagioclase-liquid hygrometry yields H₂O concentrations of 2.7-2.8 wt % for Yonaguni Graben lavas and 2.2 wt% for Yaeyama Gragen lavas (Table S8). The estimated H2O concentrations were put back into clinopyroxene-liquid thermobarometers, yielding average temperatures and pressures of \sim 1103 \pm 10 $^{\circ}$ C, \sim 3.10 \pm 0.77 kbar for Yonaguni Graben lavas and ${\sim}1063~{\pm}~11~^{\circ}\text{C},~{\sim}2.80~{\pm}~1.18$ kbar for Yaeyama Gragen lavas (Table S7). These temperatures are close to those obtained by plagioclase rims, consistent with the adiabatic magma ascent. The estimated H₂O concentrations are below the H₂O saturation in magmas under ~3 kbar (~6 wt%; Newman and Lowenstern, 2002), suggesting that the magmas are H₂O undersaturated in the reservoirs beneath the Yogaguni Graben and Yaeyama Graben.

5.1.2. Implications for the role of subducted serpentinite in water recycling Serpentinites are hydrated ultra-mafic rocks formed within the subducting slab and mantle wedge as a result of interactions between mantle rocks and seawater or fluids derived from shallow slab dehvdration (Alt et al., 2013; Deschamps et al., 2013; Scambelluri et al., 2019). Recently, serpentinites have been increasingly recognized as playing a critical role in global water recycling (e.g., Cooper et al., 2020; Kendrick et al., 2017; Ribeiro and Lee, 2017; Scambelluri et al., 2004). Firstly, serpentine minerals are enriched in H₂O (average ~13 wt%; Deschamps et al., 2013), which is much higher than H₂O in subducting sediments (~7.29 wt%; Plank, 2014) and altered oceanic crust (AOC) (~2.7 wt%; Rüpke et al., 2004). Secondly, unlike the sediments and AOC that mostly dehydrate at forearc region, serpentinite dehydration can occur at depths >200 km (Rüpke et al., 2004; Ulmer and Trommsdorff, 1995). Thus, subducted serpentinites have the potential to release significant amounts of water into the source regions of arc magmas (Rüpke

et al., 2004; Schmidt and Poli, 1998).

In the southern Okinawa Trough, an increasing contribution of serpentinite fluids to magmas was observed from the Yaeyama Graben, through the Yonuguni Graben, to the Irabu Knoll, as indicated by a gradual increase of δ^{11} B (Zhang et al., 2021a). δ^{11} B is a powerful tracer for the presence of fluids released from subducted serpentinites in arc magmas (De Hoog and Savov, 2018; Leeman et al., 2017; Scambelluri and Tonarini, 2012). This variable subduction input of serpentinite fluids is appears to be manifested in the H2O concentrations of the southern Okinawa Trough magmas. Here, we adopted H₂O/Ce ratio to evaluate the relative H2O enrichment in primitive magmas. As H2O and Ce show similar incompatibility, H₂O/Ce is not significantly affected by degree of peridotite partial melting or magma differentiation (Cartigny et al., 2008; Plank et al., 2009). This ratio is best applicable to back-arc settings, where the primitive magmas are generally water unsaturated. In contrast, because primitive arc magmas may be water saturated and potentially lose some H₂O before entrapment, the H₂O/Ce in melt inclusions should represent the minimum values of their primitive magmas.

The H₂O/Ce ratios increase from ~1000 (Yaeyama Graben) to ~1600 (Yonuguni Graben), and to ~3000 (Irabu Knoll) with increasing $\delta^{11}B$ values, which is consistent with a systematic increase of H₂O/Ce and $\delta^{11}B$ from the Mariana Trough to the Mariana Arc, and from the Lau Basin to the Tonga Arc; MORB have the lowest H₂O/Ce and $\delta^{11}B$ (Fig. 6). This robust correlation between H₂O/Ce and $\delta^{11}B$ (r² = 0.89) indicates that serpentinite-derived fluids represent a significant contribution to the water budget of arc magmas.

5.2. Volatile degassing and constraints on the magmatic contributions to the hydrothermal systems in the southern Okinawa Trough

5.2.1. Magma CO_2 degassing and its possible contribution to the hydrothermal system

Carbon isotopes ($\delta^{13}C_{PDB}\approx-8\%$ to -4%) indicate that the CO₂ dissolved in hydrothermal fluids of the Okinawa Trough has a magmatic origin (Ishibashi et al., 2014; Ishibashi and Urabe, 1995; Konno et al., 2006; Miyazaki et al., 2017; Sakai et al., 1990). The extremely low CO₂ concentrations in the matrix glasses suggest that magmas in the southern Okinawa Trough have experienced significant CO₂ degassing during ascent and eruption. This is quite different from the lavas erupted at the mid-ocean ridges, which retain relatively high concentrations of CO₂ (e. g., >100 µg/g; le Roux et al., 2006; Shaw et al., 2010; Soule et al., 2012) (Fig. 5). Our results suggest that the interaction between seawater and CO₂-poor crustal rocks is unlikely to contribute significant amounts of CO₂ into the hydrothermal system. Therefore, the high flux of CO₂ observed in vent fluids from the Okinawa Trough is most likely a result of magma degassing (Ishibashi et al., 2014; Ishibashi and Urabe, 1995; Kawagucci et al., 2011; Miyazaki et al., 2017).

The H₂O concentrations in the melt inclusions of Irabu Knoll lavas range from \sim 2.6 wt% to \sim 1.7 wt% (Fig. 5), suggesting that magmas have undergone pre-eruptive degassing in the sub-volcanic reservoir. The CO₂ concentrations in the melt inclusions decrease with the decreasing H2O concentrations, with the lowest values <10 µg/g (Fig. 5). Even if 90% of the total CO2 in these melt inclusions is sequestered in vapor bubbles, the reconstructed CO2 concentration is <50 μg/g. It is estimated that primary arc magmas have CO₂ concentrations up to $>3000 \mu g/g$ (Wallace, 2005), implying that magmas beneath the Irabu Knoll might have experienced significant CO2 degassing prior to eruption. In this case, 1 km³ of magma will release about 7.5 \times 10⁶ tons of CO₂, which can support a high CO₂ flux hydrothermal vent (200 mmol/L CO₂, with a total fluid flux of 50 L/s) for >500 years. Therefore, magma degassing in a shallow reservoir has the potential to supply enough CO2 to explain concentrations in the hydrothermal system of the Okinawa Trough.

In addition to the Okinawa Trough, CO_2 -rich hydrothermal fluids (>100 mmol/L CO_2) have been observed in other subduction-related

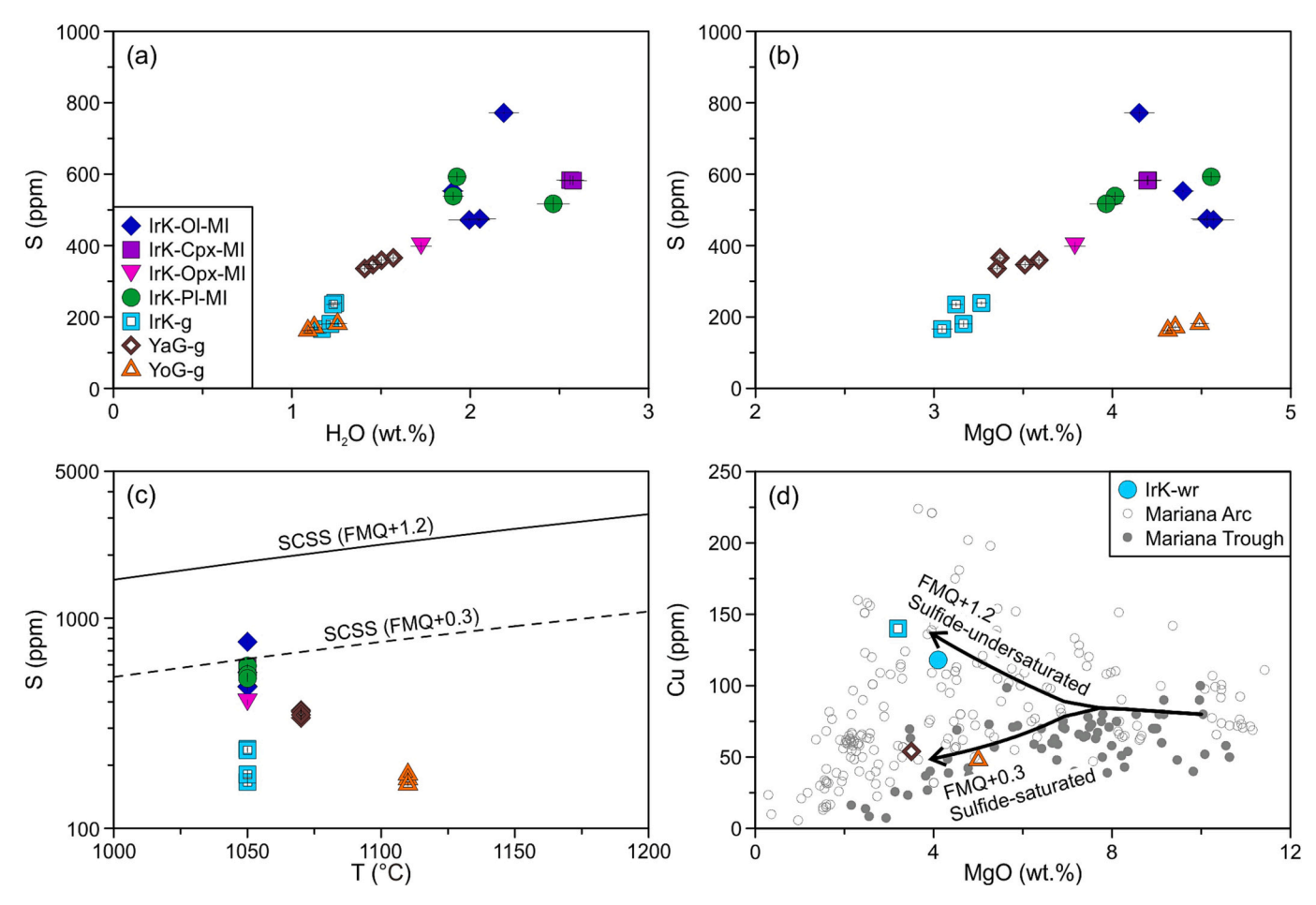


Fig. 7. Plots of S versus H_2O (a), S versus MgO (b), S versus magma temperatures (c), and Cu versus MgO (d) for the melt inclusions, matrix glasses, or lavas from the southern Okinawa Trough. The SCSS curves (at 1 kbar) in (c) are calculated using the model of Lee et al. (2012). The Cu evolution curves in (d) are calculated following the tholeiitic magma evolution model of Lee et al. (2012) at 3 kbar. The initial melt is set to contain $80 \, \mu g/g$ Cu and $1000 \, \mu g/g$ S. Change of pressure from 3 kbar to 1 kbar has little influence on the modeling results. The Cu data of Mariana Arc and Mariana Trough (from GEOROC database: http://georoc.mpch-mainz.gwd g.de/georoc/) are presented for comparison. The Mariana Arc lavas have higher f_{O2} (FMQ + 1.0 to FMQ + 1.6) than the Mariana Trough lavas (FMQ + 0.1 to FMQ + 0.6) (Brounce et al., 2014). Abbreviations: IrK-Irabu Knoll, YaG-Yaeyama Graben, YoG-Yonaguni Graben.

settings, such as the Mariana Arc (Lupton et al., 2006) and Eastern Manus Basin (Reeves et al., 2011; Seewald et al., 2019). In comparison, the hydrothermal fluids associated with mid-ocean ridges generally have much lower CO₂ concentrations (mostly <20 mmol/L; e.g., Charlou et al., 1996; Foustoukos et al., 2009; Gamo et al., 2006; Shitashima, 1998). Factors controlling the CO₂ flux of hydrothermal systems may include the amount of CO2 released during magma degassing and the efficiency of CO2 transport from a shallow magma reservoir to the overlying hydrothermal system. As primitive, undegassed magmas beneath the mid-ocean ridges are predicted to have very high concentrations of CO₂ (up to >1 wt%; Le Voyer et al., 2019), by no means can we simply conclude that less CO₂ degassing occurs in these areas relative to in convergent margins. In addition, unlike the magmas beneath the mid-ocean ridges that mainly degas CO2, subduction-related magmas can also release significant amount of other volatile species, such as H2O (Fig. 5), probably forming a CO_2 - H_2O supercritical fluid phase (Kaszuba et al., 2006). Will the presence of a fluid phase favor the transfer of exsolved CO2 into the hydrothermal system? Further experiments or numerical modeling is required to answer this question.

5.2.2. Decreasing S concentrations in the melt: S degassing or sulfide segregation?

Numerous studies have suggested injection of magmatic S into hydrothermal systems (e.g., Butterfield et al., 2011; Chen et al., 2021; Herzig et al., 1998; Kim et al., 2004; Li et al., 2019; Seewald et al., 2015;

Seewald et al., 2019; Yang and Scott, 2002; Yang and Scott, 2005). One possible mechanism for this is the transport of magmatically degassed S to the hydrothermal fluids (Butterfield et al., 2011; Seewald et al., 2015; Seewald et al., 2019). On the other hand, S can be segregated from the melt at sulfide saturation and form a sulfide mineral or immiscible sulfide liquid that is highly enriched in chalcophile metals (e.g., Cu, Au, Zn, Ag; Jenner, 2017; Patten et al., 2013). The sulfide phase will dissolve when the host melts become sulfide-undersaturated, during which S and chalcophile metals could be transferred into a fluid phase as these elements have very high fluid-melt partition coefficients (Edmonds and Mather, 2017; Nadeau et al., 2010; Simon and Ripley, 2011). Such metal-rich fluids are thought to represent a significant contribution to hydrothermal systems (Chen et al., 2021; Li et al., 2019; Yang and Scott, 1996; Yang and Scott, 2002).

The hydrothermal products in the Okinawa Trough record the input of magmatic S (Cao et al., 2018; Wang et al., 2020; Yang et al., 2020; Zeng et al., 2011). The S concentrations in melt inclusions and matrix glasses of the southern Okinawa Trough lavas decrease with the loss of $\rm H_2O$ (Fig. 7a), probably indicating a S degassing trend. However, the S concentrations in the Irabu Knoll melts also drop with decreasing MgO concentrations (Fig. 7b). Sulfide crystallization could occur during magma evolution (Lee et al., 2012), which may also account for the decrease of S concentrations in the melts. Thus, it is necessary to constrain which process controls the S behavior in the southern Okinawa Trough magmas.

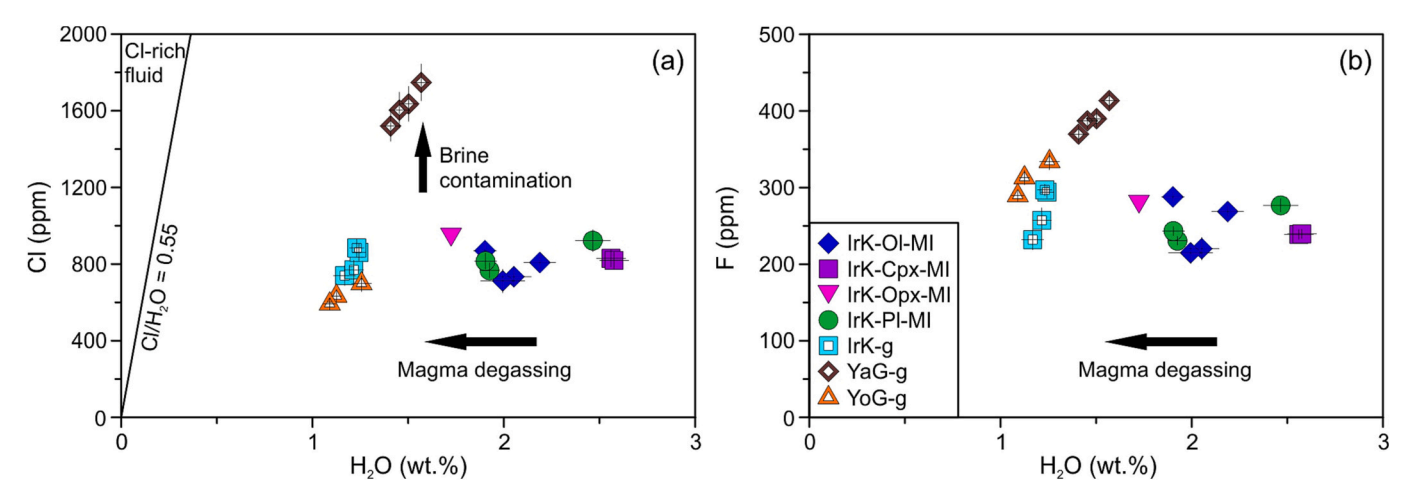


Fig. 8. Plots of Cl versus H_2O (a) and F versus H_2O (b) for the melt inclusions and matrix glasses in the southern Okinawa Trough lavas. The line in (a) indicates the minimum Cl/H_2O (0.55) for the exsolution of hydrosaline chloride liquid in basaltic magma (Webster, 2004). The much higher Cl concentrations of the Yaeyama Graben glasses is attributed to brine contamination during magma ascent (Zhang et al., 2021a). Abbreviations: IrK-Irabu Knoll, YaG-Yaeyama Graben, YoG-Yonaguni Graben.

A prerequisite for sulfide saturation is that S concentrations in magmas reach or exceed the solubility of sulfide (SCSS), which is dependent on oxygen fugacity (f_{O2}), temperature, pressure, and melt composition (e.g., Jugo et al., 2005; Mavrogenes and O'Neill, 1999; Nash et al., 2019; O'Neill and Mavrogenes, 2002). Based a SCSS model at 1 kbar and 1050 $^{\circ}$ C, and FMQ + 1.2 (FMQ: fayalite-magnetite-quartz buffer) (Lee et al., 2012), all the Irabu Knoll melt inclusions are sulfide-undersaturated (Fig. 7c). Furthermore, the Irabu Knoll lavas are characterized by high Cu concentrations (\sim 140 µg/g in matrix glasses) relative to the lavas in the Yaeyama Graben (~54 μg/g) and Yonaguni Graben (\sim 48 µg/g) (Fig. 7d). As Cu is highly compatible in sulfide, Cu concentrations in magmas are controlled by the behavior of sulfide phase (Lee et al., 2012). That means the magmas beneath the Irabu Knoll might have experienced only minor sulfide fractionation. In contrast, sulfide crystallization and re-dissolution has been reported in the Yaeyama Graben lavas (Chen et al., 2021). Previous studies suggested that sulfide saturation can be triggered by the onset of magnetite crystallization, which is favored in arcs with thicker crust (Chiaradia, 2014). However, the Yaeyama Graben has the thinnest crust in the Okinawa Trough (Arai et al., 2017; Nishizawa et al., 2019) and no significant decrease of FeO_T concentrations was observed in the Yaeyama Graben lavas (Table S5), suggesting the sulfide saturation in the southern Okinawa Trough is not related to crustal thickness and Fe depletion. Accordingly, one more plausible explanation for the transition from sulfide-undersaturated magmas in the Irabu Knoll to sulfide-saturated magmas in the Yaeyama Graben is the change of $f_{\rm O2}$, which is one of the most important controlling factors for SCSS (e.g., Jugo et al., 2005): S mainly occurs as S^{6+} at high $f_{\rm O2}$ and as S^{2-} at reduced conditions; the solubility of S^{6+} in silicate magmas is 10 times higher than that of S^{2-} . We speculate that the Yaeyama Graben magmas might have lower f_{O2} than the Irabu Knoll magmas due to the lack of subduction input of oxidizing slab-derived fluids into the back-arc mantle (Zhang et al., 2021a; Zhang et al., 2021b). This cross-arc decrease in f_{O2} has been reported in the Mariana subduction zone, where the arc lavas record higher $f_{\rm O2}$ (FMQ + 1.0 to FMQ + 1.6) than the back-arc lavas (FMQ +0.1 to FMQ + 0.6) (Brounce et al., 2014). According to a f_{O2} -controlled Cu evolution model of Lee et al. (2012), the Irabu Knoll magmas are consistent with a higher $f_{\rm O2}$ (~FMQ + 1.2) relative to the Yaeyama Graben and Yonaguni Graben magmas (\sim FMQ + 0.3) (Fig. 7d).

It is noted that the glasses of Yaeyama Graben and Yonaguni Graben lavas have S concentrations that are below sulfide saturation (Fig. 7c), suggesting that there might be other processes that sequester extra S from these melts. As S is preferentially partitioned into a vapor phase at

low pressures, S exsolution from magmas can be promoted by H2O degassing (Wallace and Edmonds, 2011). The co-variation of S and H₂O in the southern Okinawa Trough melts is thus most likely indicative of S degassing (Fig. 7a), which is considered as a major mechanism for inducing the resorption of sulfides in the Yaeyama Graben lavas (Chen et al., 2021). The melt inclusions have a minimum S concentration of \sim 400 µg/g, and the most degassed pre-eruptive magmas may contain S less than this value. Primitive arc magmas typically have S concentrations of 900-2500 µg/g (Wallace and Edmonds, 2011), implying that a significant amount of S (e.g., SO2) can be released from the magma chamber beneath the southern Okinawa Trough as a vapor and this is a potentially important source of S for the hydrothermal system. In addition to the direct input of S, the disproportionation of SO₂ can produce strong acid (H₂SO₄), which will significantly decrease the pH of hydrothermal fluids and have a significant impact on fluid-rock interactions and metals transportation (Seewald et al., 2015; Seewald et al., 2019). Furthermore, the occurrence of sulfide crystallization and re-dissolution in the Yaeyama Graben magmas might indicate a potential contribution of metal-rich magmatic fluids to the hydrothermal system in this area (Chen et al., 2021).

5.2.3. No significant Cl-F degassing

Magmatically derived halogen-bearing vapor (e.g, HCl and HF) might be injected directly into hydrothermal systems. Like SO₂, HCl and HF are highly acidic and thereby can reduce the pH and affect the dissolution and transport of metals in hydrothermal fluids (Seewald et al., 2015; Seewald et al., 2019). In addition, halogens, especially Cl, tend to partition into a fluid phase (e.g., Alletti et al., 2009; Botcharnikov et al., 2015; Webster et al., 1999; Webster et al., 2014; Webster et al., 2018). More importantly, Cl is an important ligand that is highly efficient at complexing with metals (e.g., Cu, Zn, Pb) in hydrothermal fluids (e.g., Aiuppa et al., 2009). Therefore, a hydrosaline liquid exsolved from magmas is capable of delivering metals to the hydrothermal systems.

As shown in Fig. 8, however, the concentrations of Cl and F remain nearly unchanged with the decreasing H₂O concentrations from the melt inclusions to the matrix glasses of the Irabu Knoll lavas. The higher Cl and F concentrations in the Yaeyama Graben glasses are attributed to the saline brine contamination during magma ascent (Zhang et al., 2021a). These results indicate that no significant Cl—F degassing occurs in shallow magma reservoirs and even during magma eruption in the southern Okinawa Trough. This is because F is highly soluble in silicate melt and the solubility of Cl dramatically increases in basaltic melts (up

to a few weight percent) relative to in silicic melts (Aiuppa et al., 2009; Webster et al., 1999). In such cases, F and Cl partition much less preferentially into the vapor phase compared with other volatile species (CO₂, S, H₂O), especially in basaltic melts (e.g., Brey et al., 2009; Veksler et al., 2012; Webster et al., 2015; Webster et al., 2018).

Furthermore, the melt inclusions have a Cl/ H_2O ratio of 0.03–0.05, much lower than the threshold (\sim 0.55) of hydrosaline chloride liquid exsolution in basaltic melts (Webster, 2004) (Fig. 8a). Previous study suggests that the felsic magmas in the southernmost part of the Okinawa Trough also fail to exsolve Cl-rich fluids (Chen et al., 2020). Therefore, the magmas in the southern Okinawa Trough have no contributions of Cl and F to the hydrothermal system.

6. Conclusions

We report the volatile (H_2O , CO_2 , and S) concentrations of melt inclusions and/or matrix glasses in volcanic rocks from the Irabu Knoll (modern arc front), Yaeyama Graben (back-arc), and Yonaguni Graben (back-arc) in the southern Okinawa Trough. The estimated pre-eruptive H_2O concentrations range from $\sim\!2.2$ wt% to $\sim\!3.1$ wt%, with the H_2O /Ce decreasing systematically with $\delta^{11}B$ from the arc to the back-arc. This correlation between H_2O /Ce and $\delta^{11}B$ is also observed in the Mariana and Tonga subduction zones, suggesting that subducted serpentinites might play an important role in recycling water to the sub-arc mantle.

Magmas in the southern Okinawa Trough are characterized by significant CO_2 degassing. This, on the one hand, indicates that the erupted CO_2 -depleted lavas are unlikely to be the source of CO_2 for hydrothermal fluids. On the other hand, the magmas in the shallow reservoirs can release significant amounts of CO_2 that are sufficient to support the high CO_2 flux of hydrothermal system in the Okinawa Trough. In addition, magma degassing can also release S and H_2O , but little F and Cl. Therefore, our results suggest that magma degassing is potentially an important source of CO_2 , S, and H_2O for the hydrothermal system in the Okinawa Trough.

Declaration of Competing Interest

None.

Acknowledgement

We are grateful for the crew on the HOBAB4 cruise in 2016 for their help in collecting the samples. We thank K. Guo and Z.G. Li for their comments and suggestions and D.C. Zhu for efficient editorial handling. This work was supported by the National Natural Science Foundation of China (91958213 and 42206058), the Strategic Priority Research Program (B) of Chinese Academy of Sciences (XDB42020402), the Shandong Provincial Natural Science Foundation, China (ZR2020QD068 and ZR2020MD068), the Open Fund of the Key Laboratory of Marine Geology and Environment, Chinese Academy of Sciences (Grant Nos. MGE2022KG10), the Taishan Scholars Program, and NSF OCE-2135901 to GG.

Appendix A. Supplementary data

Supplementary data to this article can be found online at https://doi.org/10.1016/j.lithos.2023.107145.

References

- Aiuppa, A., Baker, D.R., Webster, J.D., 2009. Halogens in volcanic systems. Chem. Geol. 263, 1–18.
- Alletti, M., Baker, D.R., Scaillet, B., Aiuppa, A., Moretti, R., Ottolini, L., 2009. Chlorine partitioning between a basaltic melt and H₂O–CO₂ fluids at Mount Etna. Chem. Geol. 263, 37–50.
- Alt, J.C., Schwarzenbach, E.M., Früh-Green, G.L., Shanks, W.C., Bernasconi, S.M., Garrido, C.J., Crispini, L., Gaggero, L., Padrón-Navarta, J.A., Marchesi, C., 2013. The

- role of serpentinites in cycling of carbon and sulfur: Seafloor serpentinization and subduction metamorphism. Lithos $178,\,40-54.$
- Arai, R., Kodaira, S., Yuka, K., Takahashi, T., Miura, S., Kaneda, Y., 2017. Crustal structure of the southern Okinawa Trough: Symmetrical rifting, submarine volcano, and potential mantle accretion in the continental back-arc basin. J. Geophys. Res. Solid Earth 122, 622–641.
- Botcharnikov, R.E., Holtz, F., Behrens, H., 2015. Solubility and fluid–melt partitioning of H₂O and Cl in andesitic magmas as a function of pressure between 50 and 500 MPa. Chem. Geol. 418, 117–131.
- Brey, G.P., Bulatov, V.K., Girnis, A.V., 2009. Influence of water and fluorine on melting of carbonated peridotite at 6 and 10 GPa. Lithos 112, 249–259.
- Brounce, M.N., Kelley, K.A., Cottrell, E., 2014. Variations in Fe³⁺/ \sum Fe of Mariana arc basalts and mantle wedge fO_2 . J. Petrol. 55, 2513–2536.
- Bucholz, C.E., Gaetani, G.A., Behn, M.D., Shimizu, N., 2013. Post-entrapment modification of volatiles and oxygen fugacity in olivine-hosted melt inclusions. Earth Planet. Sci. Lett. 374, 145–155.
- Butterfield, D.A., Nakamura, K.-I., Takano, B., Lilley, M.D., Lupton, J.E., Resing, J.A., Roe, K.K., 2011. High SO₂ flux, sulfur accumulation, and gas fractionation at an erupting submarine volcano. Geology 39, 803–806.
- Cao, H., Sun, Z.-L., Liu, C.-L., Liu, E.-T., Jiang, X.-J., Huang, W., 2018. Origin of natural sulfur-metal chimney in the Tangyin hydrothermal field, Okinawa Trough: constraints from rare earth element and sulfur isotopic compositions. China Geol. 1, 225–235.
- Cartigny, P., Pineau, F., Aubaud, C., Javoy, M., 2008. Towards a consistent mantle carbon flux estimate: Insights from volatile systematics (H₂O/Ce, δD, CO₂/Nb) in the North Atlantic mantle (14° N and 34° N). Earth Planet. Sci. Lett. 265, 672–685.
- Charlou, J.L., Fouquet, Y., Donval, J.P., Auzende, J.M., Jean-Baptiste, P., Stievenard, M., Michel, S., 1996. Mineral and gas chemistry of hydrothermal fluids on an ultrafast spreading ridge: East Pacific rise, 17° to 19°S (Naudur cruise, 1993) phase separation processes controlled by volcanic and tectonic activity. J. Geophys. Res. Solid Earth 101, 15899–15919.
- Chaussidon, M., Jambon, A., 1994. Boron content and isotopic composition of oceanic basalts: Geochemical and cosmochemical implications. Earth Planet. Sci. Lett. 121, 277–291.
- Chaussidon, M., Marty, B., 1995. Primitive boron isotope composition of the mantle. Science 269, 383–386.
- Chen, Z., Zeng, Z., Wang, X., Yin, X., Chen, S., Guo, K., Lai, Z., Zhang, Y., Ma, Y., Qi, H., Wu, L., 2018. U-Th/he dating and chemical compositions of apatite in the dacite from the southwestern Okinawa Trough: Implications for petrogenesis. J. Asian Earth Sci. 161. 1–13.
- Chen, Z., Zeng, Z., Qi, H., Wang, X., Yin, X., Chen, S., Yang, W., Ma, Y., Zhang, Y., 2020. Amphibole perspective to unravel the rhyolite as a potential fertile source for the Yonaguni Knoll IV hydrothermal system in the southwestern Okinawa Trough. Geol. J. 55. 4279–4301.
- Chen, Z., Zeng, Z., Tamehe, L.S., Wang, X., Chen, K., Yin, X., Yang, W., Qi, H., 2021. Magmatic sulfide saturation and dissolution in the basaltic andesitic magma from the Yaeyama Central Graben, southern Okinawa Trough. Lithos 388–389, 106082.
- Chiaradia, M., 2014. Copper enrichment in arc magmas controlled by overriding plate thickness. Nat. Geosci. 7, 43–46.
- Cooper, G.F., Macpherson, C.G., Blundy, J.D., Maunder, B., Allen, R.W., Goes, S., Collier, J.S., Bie, L., Harmon, N., Hicks, S.P., Iveson, A.A., Prytulak, J., Rietbrock, A., Rychert, C.A., Davidson, J.P., Cooper, G.F., Macpherson, C.G., Blundy, J.D., Maunder, B., Allen, R.W., Goes, S., Collier, J.S., Bie, L., Harmon, N., Hicks, S.P., Rietbrock, A., Rychert, C.A., Davidson, J.P., Davy, R.G., Henstock, T.J., Kendall, M. J., Schlaphorst, D., van Hunen, J., Wilkinson, J.J., Wilson, M., the Voi, L.A.t, 2020. Variable water input controls evolution of the Lesser Antilles volcanic arc. Nature 582, 525–529.
- Danyushevsky, L.V., McNeill, A.W., Sobolev, A.V., 2002. Experimental and petrological studies of melt inclusions in phenocrysts from mantle-derived magmas: an overview of techniques, advantages and complications. Chem. Geol. 183, 5–24.
- De Hoog, J.C.M., Savov, I.P., 2018. Boron isotopes as a tracer of subduction zone processes. In: Marschall, H., Foster, G. (Eds.), Boron Isotopes: The Fifth Element. Springer, Cham, pp. 217–247.
- Deschamps, F., Godard, M., Guillot, S., Hattori, K., 2013. Geochemistry of subduction zone serpentinites: a review. Lithos 178, 96–127.
- Edmonds, M., Mather, T.A., 2017. Volcanic sulfides and outgassing. Elements 13, 105-110.
- Foustoukos, D.I., Pester, N.J., Ding, K., Seyfried Jr., W.E., 2009. Dissolved carbon species in associated diffuse and focused flow hydrothermal vents at the Main Endeavour Field, Juan de Fuca Ridge: phase equilibria and kinetic constraints. Geochem. Geophys. Geosyst. 10. Q10003.
- Fukuba, T., Noguchi, T., Fujii, T., 2015. The Irabu Knoll: Hydrothermal site at the eastern edge of the Yaeyama Graben. In: Ishibashi, J.-I., Okino, K., Sunamura, M. (Eds.), Subseafloor Biosphere Linked to Hydrothermal Systems: TAIGA Concept. Springer, Japan, Tokyo, pp. 493–496.
- Gaetani, G.A., O'Leary, J.A., Shimizu, N., Bucholz, C.E., Newville, M., 2012. Rapid reequilibration of $\rm H_2O$ and oxygen fugacity in olivine-hosted melt inclusions. Geology 40, 915–918.
- Gamo, T., Ishibashi, J., Tsunogai, U., Okamura, K., Chiba, H., 2006. Unique geochemistry of submarine hydrothermal fluids from arc-back-arc settings of the Western Pacific. In: Christie, D.M., Fisher, C.R., Lee, S.-M., Givens, S. (Eds.), Back-Arc Spreading Systems: Geological, Biological, Chemical, and Physical Interactions. American Geophysical Union, Washington, DC, pp. 147–161.
- Glasby, G.P., Notsu, K., 2003. Submarine hydrothermal mineralization in the Okinawa Trough, SW of Japan: an overview. Ore Geol. Rev. 23, 299–339.

- Guo, K., Zeng, Z., Chen, S., Zhang, Y., Qi, H., Ma, Y., 2017. The influence of a subduction component on magmatism in the Okinawa Trough: evidence from thorium and related trace element ratios. J. Asian Earth Sci. 145 (Part A), 205–216.
- Halbach, P., Pracejus, B., Maerten, A., 1993. Geology and mineralogy of massive sulfide ores from the Central Okinawa Trough, Japan. Econ. Geol. 88, 2210–2225.
- Herzig, P.M., Hannington, M.D., Arribas Jr., A., 1998. Sulfur isotopic composition of hydrothermal precipitates from the Lau back-arc: Implications for magmatic contributions to seafloor hydrothermal systems. Mineral. Deposita 33, 226–237.
- Hou, Z., Khin, Z., Li, Y., Zhang, Q., Zeng, Z., Tetsuro, U., 2005. Contribution of magmatic fluid to the active hydrothermal system in the JADE field, Okinawa Trough: evidence from fluid inclusions, oxygen and helium isotopes. Int. Geol. Rev. 47, 420–437.
- Ishibashi, J.I., Urabe, T., 1995. Hydrothermal activity related to arc-backarc magmatism in the Western Pacific. In: Taylor, B. (Ed.), Back Arc Basins. Plenum Press, New York, pp. 451–495.
- Ishibashi, J.I., Noguchi, T., Toki, T., Miyabe, S., Yamagami, S., Onishi, Y., Yamanaka, T., Yokoyama, Y., Omori, E., Takahashi, Y., 2014. Diversity of fluid geochemistry affected by processes during fluid upwelling in active hydrothermal fields in the Izena Hole, the middle Okinawa Trough back-arc basin. Geochem. J. 48, 357–369.
- Ishikawa, T., Tera, F., 1999. Two isotopically distinct fluid components involved in the Mariana arc: evidence from Nb/B ratios and B, Sr, Nd, and Pb isotope systematics. Geology 27, 83–86.
- Jenner, F.E., 2017. Cumulate causes for the low contents of sulfide-loving elements in the continental crust. Nat. Geosci. 10, 524–529.
- Jugo, P.J., Luth, R.W., Richards, J.P., 2005. Experimental data on the speciation of sulfur as a function of oxygen fugacity in basaltic melts. Geochim. Cosmochim. Acta 69, 497–503.
- Kaszuba, J.P., Williams, L.L., Janecky, D.R., Hollis, W.K., Tsimpanogiannis, I.N., 2006. Immiscible CO₂-H₂O fluids in the shallow crust. Geochem. Geophys. Geosyst. 7. 010003
- Kawagucci, S., Chiba, H., Ishibashi, J.-I., Yamanaka, T., Toki, T., Muramatsu, Y., Ueno, Y., Makabe, A., Inoue, K., Yoshida, N., 2011. Hydrothermal fluid geochemistry at the Iheya North field in the mid-Okinawa Trough: Implication for origin of methane in subseafloor fluid circulation systems. Geochem. J. 45, 109–124.
- Kendrick, M.A., Hémond, C., Kamenetsky, V.S., Danyushevsky, L., Devey, C.W., Rodemann, T., Jackson, M.G., Perfit, M.R., 2017. Seawater cycled throughout Earth's mantle in partially serpentinized lithosphere. Nat. Geosci. 10, 222–228.
- Kendrick, M.A., Danyushevsky, L.V., Falloon, T.J., Woodhead, J.D., Arculus, R.J., Ireland, T., 2020. SW Pacific arc and backarc lavas and the role of slab-bend serpentinites in the global halogen cycle. Earth Planet. Sci. Lett. 530, 115921.
- Kim, J., Lee, I., Lee, K.-Y., 2004. S, Sr, and Pb isotopic systematics of hydrothermal chimney precipitates from the Eastern Manus Basin, western Pacific: Evaluation of magmatic contribution to hydrothermal system. J. Geophys. Res. Solid Earth 109. B12210.
- Kim, J., Lee, K.-Y., Kim, J.-H., 2011. Metal-bearing molten sulfur collected from a submarine volcano: Implications for vapor transport of metals in seafloor hydrothermal systems. Geology 39, 351–354.
- Konno, U., Tsunogai, U., Nakagawa, F., Nakaseama, M., Ishibashi, J.-I., Nunoura, T., Nakamura, K.-I., 2006. Liquid CO₂ venting on the seafloor: Yonaguni Knoll IV hydrothermal system, Okinawa Trough. Geophys. Res, Lett. 33. L16607.
- le Roux, P.J., Shirey, S.B., Hauri, E.H., Perfit, M.R., Bender, J.F., 2006. The effects of variable sources, processes and contaminants on the composition of northern EPR MORB (8–10°N and 12–14°N): evidence from volatiles (H₂O, CO₂, S) and halogens (F. Cl). Earth Planet. Sci. Lett. 251, 209–231.
- Le Voyer, M., Hauri, E.H., Cottrell, E., Kelley, K.A., Salters, V.J.M., Langmuir, C.H., Hilton, D.R., Barry, P.H., Füri, E., 2019. Carbon fluxes and primary magma CO₂ contents along the global mid-ocean ridge system. Geochem. Geophys. Geosyst. 20, 1387–1424.
- Lee, C.-T.A., Luffi, P., Chin, E.J., Bouchet, R., Dasgupta, R., Morton, D.M., Le Roux, V., Yin, Q.-Z., Jin, D., 2012. Copper systematics in arc magmas and implications for crust-mantle differentiation. Science 336, 64–68.
- Leeman, W.P., Tonarini, S., Turner, S., 2017. Boron isotope variations in Tonga-Kermadec-New Zealand arc lavas: Implications for the origin of subduction components and mantle influences. Geochem. Geophys. Geosyst. 18, 1126–1162.
- Li, Z., Chu, F., Zhu, J., Ding, Y., Zhu, Z., Liu, J., Wang, H., Li, X., Dong, Y., Zhao, D., 2019. Magmatic sulfide formation and oxidative dissolution in the SW Okinawa Trough: a precursor to metal-bearing magmatic fluid. Geochim. Cosmochim. Acta 258, 138-155
- Lupton, J., Butterfield, D., Lilley, M., Evans, L., Nakamura, K.-I., Chadwick Jr., W., Resing, J., Embley, R., Olson, E., Proskurowski, G., Baker, E., de Ronde, C., Roe, K., Greene, R., Lebon, G., Young, C., 2006. Submarine venting of liquid carbon dioxide on a Mariana Arc volcano. Geochem. Geophys. Geosyst. 7. Q08007.
- Marques, A.F.A., Scott, S.D., Guillong, M., 2011. Magmatic degassing of ore-metals at the Menez Gwen: Input from the Azores plume into an active Mid-Atlantic Ridge seafloor hydrothermal system. Earth Planet. Sci. Lett. 310, 145–160.
- Marschall, H.R., 2018. Boron isotopes in the ocean floor realm and the mantle. In: Marschall, H., Foster, G. (Eds.), Boron Isotopes: The Fifth Element. Springer, Cham, pp. 189–215.
- Mavrogenes, J.A., O'Neill, H.S.C., 1999. The relative effects of pressure, temperature and oxygen fugacity on the solubility of sulfide in mafic magmas. Geochim. Cosmochim. Acta 63, 1173–1180.
- Miyazaki, J., Kawagucci, S., Makabe, A., Takahashi, A., Kitada, K., Torimoto, J., Matsui, Y., Tasumi, E., Shibuya, T., Nakamura, K., Horai, S., Sato, S., Ishibashi, J.-I., Kanzaki, H., Nakagawa, S., Hirai, M., Takaki, Y., Okino, K., Watanabe, H.K., Kumagai, H., Chen, C., 2017. Deepest and hottest hydrothermal activity in the Okinawa Trough: the Yokosuka site at Yaeyama Knoll. R. Soc. Open Sci. 4, 171570.

Moore, L.R., Gazel, E., Tuohy, R., Lloyd, A.S., Esposito, R., Steele-MacInnis, M., Hauri, E. H., Wallace, P.J., Plank, T., Bodnar, R.J., 2015. Bubbles matter: an assessment of the contribution of vapor bubbles to melt inclusion volatile budgets. Am. Mineral. 100, 806–823.

- Nadeau, O., Williams-Jones, A.E., Stix, J., 2010. Sulphide magma as a source of metals in arc-related magmatic hydrothermal ore fluids. Nat. Geosci. 3, 501–505.
- Nash, W.M., Smythe, D.J., Wood, B.J., 2019. Compositional and temperature effects on sulfur speciation and solubility in silicate melts. Earth Planet. Sci. Lett. 507, 187-198
- Newman, S., Lowenstern, J.B., 2002. VolatileCalc: a silicate $melt-H_2O-CO_2$ solution model written in Visual basic for excel. Comput. Geosci. 28, 597–604.
- Nishizawa, A., Kaneda, K., Oikawa, M., Horiuchi, D., Fujioka, Y., Okada, C., 2019. Seismic structure of rifting in the Okinawa Trough, an active backarc basin of the Ryukyu (Nansei-Shoto) island arc–trench system. Earth Planets Space 71, 21.
- O'Neill, H.S.C., Mavrogenes, J.A., 2002. The sulfide capacity and the sulfur content at sulfide saturation of silicate melts at 1400°C and 1 bar. J. Petrol. 43, 1049–1087.
- Patten, C., Barnes, S.-J., Mathez, E.A., Jenner, F.E., 2013. Partition coefficients of chalcophile elements between sulfide and silicate melts and the early crystallization history of sulfide liquid: LA-ICP-MS analysis of MORB sulfide droplets. Chem. Geol. 358, 170–188.
- Plank, T., 2014. The chemical composition of subducting sediments. In: Keeling, R.F. (Ed.), Treatise on Geochemistry. Elsevier, Amsterdam, pp. 607–629.
- Plank, T., Cooper, L.B., Manning, C.E., 2009. Emerging geothermometers for estimating slab surface temperatures. Nat. Geosci. 2, 611–615.
- Putirka, K.D., 2008. Thermometers and barometers for volcanic systems. Rev. Mineral. Geochem. 69, 61–120.
- Rasmussen, D.J., Plank, T.A., Wallace, P.J., Newcombe, M.E., Lowenstern, J.B., 2020. Vapor-bubble growth in olivine-hosted melt inclusions. Am. Mineral. 105, 1898–1919.
- Reeves, E.P., Seewald, J.S., Saccocia, P., Bach, W., Craddock, P.R., Shanks, W.C., Sylva, S. P., Walsh, E., Pichler, T., Rosner, M., 2011. Geochemistry of hydrothermal fluids from the PACMANUS, Northeast Pual and Vienna Woods hydrothermal fields, Manus Basin, Papua New Guinea. Geochim. Cosmochim. Acta 75, 1088–1123.
- Ribeiro, J.M., Lee, C.-T.A., 2017. An imbalance in the deep water cycle at subduction zones: the potential importance of the fore-arc mantle. Earth Planet. Sci. Lett. 479, 298–309.
- Rüpke, L.H., Morgan, J.P., Hort, M., Connolly, J.A.D., 2004. Serpentine and the subduction zone water cycle. Earth Planet. Sci. Lett. 223, 17–34.
- Ruscitto, D.M., Wallace, P.J., Cooper, L.B., Plank, T., 2012. Global variations in H₂O/Ce: 2. Relationships to arc magma geochemistry and volatile fluxes. Geochem. Geophys. Geosyst. 13. Q03025.
- Sakai, H., Gamo, T., Kim, E.S., Tsutsumi, M., Tanaka, T., Ishibashi, J., Wakita, H., Yamano, M., Oomori, T., 1990. Venting of carbon dioxide-rich fluid and hydrate formation in Mid-Okinawa Trough Backarc Basin. Science 248, 1093–1096.
- Scambelluri, M., Tonarini, S., 2012. Boron isotope evidence for shallow fluid transfer across subduction zones by serpentinized mantle. Geology 40, 907–910.
- Scambelluri, M., Fiebig, J., Malaspina, N., Müntener, O., Pettke, T., 2004. Serpentinite subduction: Implications for fluid processes and trace-element recycling. Int. Geol. Rev. 46, 595–613.
- Scambelluri, M., Cannaò, E., Gilio, M., 2019. The water and fluid-mobile element cycles during serpentinite subduction. A review. Eur. J. Mineral. 31, 405–428.
- Schmidt, M.W., Poli, S., 1998. Experimentally based water budgets for dehydrating slabs and consequences for arc magma generation. Earth Planet. Sci. Lett. 163, 361–379. Seewald, J.S., Reeves, E.P., Bach, W., Saccocia, P.J., Craddock, P.R., Shanks, W.C.,
- Sylva, S.P., Pichler, T., Rosner, M., Walsh, E., 2015. Submarine venting of magmatic volatiles in the Eastern Manus Basin, Papua New Guinea. Geochim. Cosmochim. Acta 163. 178–199.
- Seewald, J.S., Reeves, E.P., Bach, W., Saccocia, P.J., Craddock, P.R., Walsh, E., Shanks, W.C., Sylva, S.P., Pichler, T., Rosner, M., 2019. Geochemistry of hot-springs at the SuSu Knolls hydrothermal field, Eastern Manus Basin: Advanced argillic alteration and vent fluid acidity. Geochim. Cosmochim. Acta 255, 25–48.
- Shaw, A.M., Hauri, E.H., Fischer, T.P., Hilton, D.R., Kelley, K.A., 2008. Hydrogen isotopes in Mariana arc melt inclusions: Implications for subduction dehydration and the deep-Earth water cycle. Earth Planet. Sci. Lett. 275, 138–145.
- Shaw, A.M., Behn, M.D., Humphris, S.E., Sohn, R.A., Gregg, P.M., 2010. Deep pooling of low degree melts and volatile fluxes at the 85 °E segment of the Gakkel Ridge: evidence from olivine-hosted melt inclusions and glasses. Earth Planet. Sci. Lett. 289, 311–322.
- Shinjo, R., Kato, Y., 2000. Geochemical constraints on the origin of bimodal magmatism at the Okinawa Trough, an incipient back-arc basin. Lithos 54, 117–137.
- Shinjo, R., Chung, S.L., Kato, Y., Kimura, M., 1999. Geochemical and Sr-Nd isotopic characteristics of volcanic rocks from the Okinawa Trough and Ryukyu Arc: Implications for the evolution of a young, intracontinental back arc basin. J. Geophys. Res. Solid Earth 104, 10591–10608.
- Shitashima, K., 1998. CO_2 supply from deep-sea hydrothermal systems. Waste Manag. 17, 385–390.
- Shu, Y., Nielsen, S.G., Zeng, Z., Shinjo, R., Blusztajn, J., Wang, X., Chen, S., 2017. Tracing subducted sediment inputs to the Ryukyu arc-Okinawa Trough system: evidence from thallium isotopes. Geochim. Cosmochim. Acta 217, 462–491.
- Sibuet, J.C., Deffontaines, B., Hsu, S.K., Thareau, N., Formal, L., Liu, C.S., 1998. Okinawa Trough backarc basin: early tectonic and magmatic evolution. J. Geophys. Res. Solid Earth 103, 30245–30267.
- Siegburg, M., Klügel, A., Rocholl, A., Bach, W., 2018. Magma plumbing and hybrid magma formation at an active back-arc basin volcano: North Su, eastern Manus basin. J. Volcanol. Geotherm. Res. 362, 1–16.

Simon, A.C., Ripley, E.M., 2011. The role of magmatic sulfur in the formation of ore deposits. Rev. Mineral. Geochem. 73, 513–578.

- Sobolev, A.V., Chaussidon, M., 1996. $\rm H_2O$ concentrations in primary melts from suprasubduction zones and mid-ocean ridges: Implications for $\rm H_2O$ storage and recycling in the mantle. Earth Planet. Sci. Lett. 137, 45–55.
- Soule, S.A., Nakata, D.S., Fornari, D.J., Fundis, A.T., Perfit, M.R., Kurz, M.D., 2012. CO₂ variability in mid-ocean ridge basalts from syn-emplacement degassing: Constraints on eruption dynamics. Earth Planet. Sci. Lett. 327–328, 39–49.
- Ulmer, P., Trommsdorff, V., 1995. Serpentine stability to mantle depths and subduction-related magmatism. Science 268, 858–861.
- Veksler, I.V., Dorfman, A.M., Dulski, P., Kamenetsky, V.S., Danyushevsky, L.V., Jeffries, T., Dingwell, D.B., 2012. Partitioning of elements between silicate melt and immiscible fluoride, chloride, carbonate, phosphate and sulfate melts, with implications to the origin of natrocarbonatite. Geochim. Cosmochim. Acta 79, 20-40
- Wallace, P.J., 2005. Volatiles in subduction zone magmas: concentrations and fluxes based on melt inclusion and volcanic gas data. J. Volcanol. Geotherm. Res. 140, 217–240.
- Wallace, P.J., Edmonds, M., 2011. The sulfur budget in magmas: evidence from melt inclusions, submarine glasses, and volcanic gas emissions. Rev. Mineral. Geochem. 73, 215–246
- Wallace, P.J., Kamenetsky, V.S., Cervantes, P., 2015. Melt inclusion $\rm CO_2$ contents, pressures of olivine crystallization, and the problem of shrinkage bubbles‡. Am. Mineral. 100, 787–794.
- Wang, H., Chu, F., Li, X., Dong, Y., Zhu, J., Li, Z., Zhu, Z., Li, J., Chen, L., 2020. Mineralogy, geochemistry, and Sr-Pb and in situ S isotopic compositions of hydrothermal precipitates from the Tangyin hydrothermal field, southern Okinawa Trough: Evaluation of the contribution of magmatic fluids and sediments to hydrothermal systems. Ore Geol. Rev. 126, 103742.
- Waters, L.E., Lange, R.A., 2015. An updated calibration of the plagioclase-liquid hygrometer-thermometer applicable to basalts through rhyolites. Am. Mineral. 100, 2172–2184.
- Webster, J.D., 2004. The exsolution of magmatic hydrosaline chloride liquids. Chem. Geol. 210, 33–48.
- Webster, J.D., Kinzler, R.J., Mathez, E.A., 1999. Chloride and water solubility in basalt and andesite melts and implications for magmatic degassing. Geochim. Cosmochim. Acta 63, 729–738.
- Webster, J.D., Goldoff, B., Sintoni, M.F., Shimizu, N., De Vivo, B., 2014. C–O–H–Cl–S–F volatile solubilities, partitioning, and mixing in phonolitic–trachytic melts and aqueous–carbonic vapor \pm saline liquid at 200 MPa. J. Petrol. 55, 2217–2248.

Webster, J.D., Vetere, F., Botcharnikov, R.E., Goldoff, B., McBirney, A., Doherty, A.L., 2015. Experimental and modeled chlorine solubilities in aluminosilicate melts at 1 to 7000 bars and 700 to 1250 °C: applications to magmas of Augustine Volcano, Alaska. Am. Mineral. 100, 522–535.

- Webster, J.D., Baker, D.R., Aiuppa, A., 2018. Halogens in Mafic and Intermediate-Silica Content Magmas. In: Harlov, D.E., Aranovich, L. (Eds.), The Role of Halogens in Terrestrial and Extraterrestrial Geochemical Processes: Surface, Crust, and Mantle. Springer International Publishing, Cham, pp. 307–430.
- Yang, K., Scott, S.D., 1996. Possible contribution of a metal-rich magmatic fluid to a seafloor hydrothermal system. Nature 383, 420–423.
- Yang, K., Scott, S.D., 2002. Magmatic degassing of volatiles and ore metals into a hydrothermal system on the modern sea floor of the Eastern Manus Back-Arc Basin, Western Pacific. Econ. Geol. 97, 1079–1100.
- Yang, K., Scott, S.D., 2005. Vigorous exsolution of volatiles in the magma chamber beneath a hydrothermal system on the modern sea floor of the Eastern Manus Back-Arc Basin, Western Pacific: evidence from melt inclusions. Econ. Geol. 100, 1005, 1006.
- Yang, B., Liu, J., Shi, X., Zhang, H., Wang, X., Wu, Y., Fang, X., 2020. Mineralogy and sulfur isotope characteristics of metalliferous sediments from the Tangyin hydrothermal field in the southern Okinawa Trough. Ore Geol. Rev. 120, 103464.
- Zellmer, G.F., Edmonds, M., Straub, S.M., 2015. Volatiles in subduction zone magmatism. Geol. Soc. Lond., Spec. Publ. 410, 1–17.
- Zeng, Z., Chen, C.-T.A., Yin, X., Zhang, X., Wang, X., Zhang, G., Wang, X., Chen, D., 2011. Origin of native sulfur ball from the Kueishantao hydrothermal field offshore Northeast Taiwan: evidence from trace and rare earth element composition. J. Asian Earth Sci. 40, 661–671.
- Zhang, Y., Zeng, Z., Chen, S., Wang, X., Yin, X., 2018. New insights into the origin of the bimodal volcanism in the middle Okinawa Trough: not a basalt-rhyolite differentiation process. Front. Earth Sci. 12, 325–338.
- Zhang, Y., Zeng, Z., Gaetani, G., Zhang, L., Lai, Z., 2020. Mineralogical constraints on the magma mixing beneath the iheya graben, an active back-arc spreading center of the Okinawa trough. J. Petrol. 61 egaa098.
- Zhang, Y., Gaetani, G., Zeng, Z., Monteleone, B., Yin, X., Wang, X., Chen, S., 2021a. Halogen (F, Cl) concentrations and Sr-Nd-Pb-B isotopes of the basaltic andesites from the southern Okinawa Trough: Implications for the recycling of subducted serpentinites. J. Geophys. Res. Solid Earth 126 e2021JB021709.
- Zhang, Y., Gazel, E., Gaetani, G.A., Klein, F., 2021b. Serpentinite-derived slab fluids control the oxidation state of the subarc mantle. Sci. Adv. 7 eabi2515.
- Zhu, Z., Ding, Y., Li, Z., Dong, Y., Wang, H., Liu, J., Zhu, J., Li, X., Chu, F., Jin, X., 2021. Hafnium isotopic constraints on crustal assimilation in response to the tectono–magmatic evolution of the Okinawa Trough. Lithos 398–399, 106352.